Dalton Transactions

Accepted Manuscript

ROYAL SOCIETY OF CHEMISTRY

www.rsc.org/dalton

$SnGa_2GeS_6$: Synthesis, Structure, Linear and Nonlinear Optical Properties

Zuohong Lin,[abc] Chao Li,[abc] Lei Kang,[abc] Zheshuai Lin,[ab] Jiyong Yao[ab,*] and Yicheng Wu[ab]

A new sulfide, $SnGa_2GeS_6$, has been synthesized, which represents the first member in the quaternary Sn/M/M'/Q (M = Ga, In; M' = Si, Ge; Q = S, Se, Te) system. It adopts a new structure type in the non-centrosymmetric space group *Fdd2*. In the structure, Sn^{2+} is coordinated to a distorted square-pyramid of five S atoms, demonstrating the stereochemical activity of electron lone pair, while the Ge atom and Ga atom are both tetrahedrally coordinated with four S atoms. The SnS_5 square-pyramids and the MS_4 (M = Ga, Ge) tetrahedra are connected to each other via corner and edge-sharing to generate a three-dimensional framework. The compound exhibits a powder second harmonic generation signal at 2 μm whose strength is about one-fourth that of the benchmark material $AgGaS_2$, which may be explained in view

[a] *Center for Crystal Research and Development, Technical Institute of Physics and Chemistry, Chinese Academy of Sciences, Beijing 100190, P.R. China*

[b] *Key Laboratory of Functional Crystals and Laser Technology, Technical Institute of Physics and Chemistry, Chinese Academy of Sciences, Beijing 100190, China, Email: jyao@mail.ipc.ac.cn*

[c] *University of Chinese Academy of Sciences, Beijing 100049, China,*

†Electronic supplementary information (ESI) available: Crystallographic data in CIF format for $SnGa_2GeS_6$.

of the macroscopic arrangement of the SnS_5 square-pyramids and the MS_4 tetrahedra. Moreover, based on UV-vis-NIR spectroscopy measurement and the electronic structure calculations, $SnGa_2GeS_6$ has two optical transitions at about 1.12 eV and 2.04 eV respectively.

Introduction

The research on metal chalcogenides has been very active for decades owing to their amazing compositional and structural complexity and also their fascinating magnetic, superconducting, thermoelectric, photocatalytic, and nonlinear optical (NLO) properties.[1–15] Recently, metal chalcogenides containing the group 14 element Sn have received much interest.[16–21] Sn atom can be stabilized at both the +2 oxidation state with an electron lone pair and at the +4 oxidation state without the electron lone pair, and its coordination environment can range from 3-fold trigonal pyramids, 4-fold tetrahedra, 5-fold square pyramids, and to 6-fold octahedra in chalcogenides. The mixed valence property and the diverse coordination environment of Sn will certainly increase the stoichiometric and structural richness of resultant compounds, and hence may lead to interesting properties.

The recent hard work in exploring new Sn-containing metal chalcogenides has led to fruitful results. A number of related compounds have been discovered, including R_2SnS_5 (R = Pr, Nd, Gd, and Tb),[16] Li_2CdSnS_4,[17] $EuCu_2SnS_4$,[18] $Ba_7Sn_5S_{15}$,[19] $BaSn_2S_5$,[19] $Ba_6Sn_7S_{20}$,[19] $In_4Pb_xSn_ySe_3$,[20] $Ba_6Sn_6Se_{13}$[21] and $SnGa_4Q_7$ (Q = S, Se).[22] Among them, $In_4Pb_xSn_ySe_3$ is a promising mid-temperature thermoelectric material with a Figure of Merit ZT = 1.4 at 733K.[20] $Ba_7Sn_5S_{15}$ possesses both the Sn_2S_3 trigonal-bipyramids and the SnS_4 tetrahedra and shows a strong NLO effect.[19] Another compound $Ba_6Sn_6Se_{13}$ exhibits the simultaneous presence of the trigonal-pyramidally coordinated Sn^{2+}, square-pyramidally coordinated Sn^{2+}, and tetrahedrally coordinated Sn^{4+} for the first time and their macroscopic packing gives

$Ba_6Sn_6Se_{13}$ a moderate NLO effect.[21]

In this paper, we focus on the quaternary Sn/M/M'/Q (M = Ga, In; M' = Si, Ge; Q = S, Se, Te) system, hoping to identify new IR NLO materials by combining the two kinds of microscopic NLO active units, namely the tetrahedral $M/M'Q_4$ units and the polyhedra centered by cations with electron lone pair (Sn^{2+}) in one compound. Our efforts led to the discovery of $SnGa_2GeS_6$, the first member in this system, which adopts a new structure type in the non-centrosymmetric space group *Fdd2*. In the structure, Sn is in the +2 oxidation state with a lone pair of electrons, whose stereochemical activity results in a square-pyramidal environment for Sn. The Ga and Ge atoms are in the usual tetrahedral environments. The macroscopic packing of these two kinds of building blocks gives rise to a moderate NLO response for $SnGa_2GeS_6$. In this work we present the synthesis, structural characterization, optical and electronic properties of $SnGa_2GeS_6$.

Experimental Section

Syntheses

The following reagents were used as obtained: Sn (Sinopharm Chemical Reagent Co., Ltd., 99.9%), Ga (Sinopharm Chemical Reagent Co., Ltd., 99.99%), Ge (Sinopharm Chemical Reagent Co., Ltd, 99.99%), S (Sinopharm Chemical Reagent Co., Ltd, 99.99%). The binary starting materials SnS, Ga_2S_3, and GeS_2 were synthesized by the stoichiometric reactions of elements at high temperatures in sealed silica tubes evacuated to 10^{-3} Pa. These reagents are all powders in the mesh size of

about 150-200 mesh.

Crystal growth of $SnGa_2GeS_6$

Reaction mixtures of 0.5 mmol of SnS, 0.5 mmol of Ga_2S_3, and 0.5 mmol of GeS_2 were ground and loaded into fused-silica tubes under an Ar atmosphere in a glovebox. The tubes were flame-sealed under a high vacuum of 10^{-3} Pa and then placed in a computer−controlled furnace. The samples were heated to 1273 K within 15 h, kept for 70 h, then slowly cooled to 573 K at the rate of 3 K/h, and finally cooled to room temperature by switching off the furnace. The resultant dark-red air-stable crystals were hand-picked from the ampoules for analysis. EDX measurement with the use of a Hitachi S-4800 SEM indicated the presence of Sn, Ga, Ge, and S in the approximate ratio of 1:2:1:6, which agreed with the single crystal X-ray structure analysis results.

Structure Determination

Single-crystal X-ray diffraction measurement was performed on a Rigaku AFC10 diffractometer equipped with a graphite- monochromated Mo K_α (λ = 0.71073 Å) radiation at 153 K. The collection of the intensity data, cell refinement and data reduction were carried out with the program Crystalclear.[23] Face-indexed absorption correction was performed numerically with the use of the program XPREP.[24]

The structure was solved with the direct methods SHELXTLS program and refined with the least-squares program SHELXL of the SHELXTL.PC suite of

programs.[24] Six S atoms and one Sn atom at general positions (Wyckoff position 16*b*) can be readily assigned according to the analysis of the difference electron density map and the coordination environment. There are four other metal positions (M1, M2 at Wyckoff positions 16*b* and M3, M4 at Wyckoff position 8*a*) in tetrahedral environments, which should be occupied by the Ga and Ge atoms. It is difficult for X-ray to differentiate between Ga and Ge atoms, thus the Ga and Ge were assigned as disordered at these four positions with a ratio of Ga:Ge = 2:1, agreeing with the EDX measurement results. The final refinements included anisotropic displacement parameters and a secondary extinction correction. Additional experimental details are given in Table 1 and selected metrical data are given in Table 2. Further information can be found in Supplementary Information.

Diffuse Reflectance Spectroscopy and XRD

Single crystals of $SnGa_2GeS_6$ (about 0.5 g) were hand-picked from reaction products and ground to powder. Then a Cary 5000 UV-vis-NIR spectrophotometer with a diffuse reflectance accessory was used to measure the spectrum of $SnGa_2GeS_6$ over the range 350 nm (3.54 eV) to 2000 nm (0.62 eV).

X-ray powder diffraction analysis of ground $SnGa_2GeS_6$ crystals was performed at room temperature in the range of $2\theta = 10–70^{o}$ with a scan step width of 0.02^{o} and a fixed counting time of 0.1 s/step using a Rigaku MiniFlex II diffractometer (Cu Kα radiation, λ = 1.5406 Å) at 153 K. The experimental powder X-ray diffraction pattern was consistent with the calculated one (Figure 1), which proves the purity of the bulk

sample.

Second Harmonic Generation (SHG) Measurement

The optical SHG response of $SnGa_2GeS_6$ was measured by means of the Kurtz-Perry method.[25] The fundamental light was the 2090 nm light generated with a Q-switched Ho:Tm:Cr:YAG laser. The particle size of the sieved sample was 80–100 μm. Homemade microcrystalline $AgGaS_2$ of similar particle size served as a reference.

Theoretical Calculation

The first-principles calculations at the atomic level for the $SnGa_2GeS_6$ crystal, including the band structure, total and partial density of states (DOS and PDOS), and the optical properties, were performed by the plane-wave pseudopotential method[26] implemented in the CASTEP program[27] based on density functional theory (DFT).[28] The exchange-correlation (XC) functionals is described by the local density approximation (LDA).[29] The ion-electron interactions are modeled by the ultrasoft pseudopotentials[30] for all constituent elements. In this model, Sn $5s^25p^2$, Ge $4s^24p^2$, Ga $3d^{10}4s^24p^1$, and S $3s^23p^4$ electrons are treated as the valence electrons, respectively. The kinetic energy cutoff of 330 eV and Monkhorst-Pack *k*-point meshes[31] spanning less than 0.04/Å^3 in the Brillouin zone is chosen to ensure the sufficient accuracy of the present purpose. Meanwhile, atomic positions in unit cell of $SnGa_2GeS_6$ are fully optimized using the quasi-Newton method[32] under fixed cell parameters. The

convergence thresholds between optimization cycles for energy change, maximum force, maximum stress, and maximum displacement are set as 5.0×10^{-6} eV per atom, 0.01 eV per Å, 0.02 GPa, and 5.0×10^{-4} Å, respectively. The optimization terminates when all of these criteria are satisfied.

Results and Discussion

Crystal Growth

The sulfide $SnGa_2GeS_6$ have been obtained by spontaneous nucleation method for the first time, representing the first member in the Sn/M/M'/Q (M = Ga, In; M' = Si, Ge; Q = S, Se, Te) system. We also tried to synthesize the selenide and telluride analogues. Unfortunately, the suspected $SnGa_2GeSe_6$ crystal was of poor quality and no analogous telluride was found. Thus we only report the study on $SnGa_2GeS_6$ here.

Crystal Structure of $SnGa_2GeS_6$

The $SnGa_2GeS_6$ compound crystallizes in the non-centrosymmetric space group *Fdd2* of the orthorhombic system with unit cell parameters of a = 45.366(9) Å, b = 7.2288(14) Å, c = 11.607(2) Å, and Z = 16. The asymmetric unit contains one crystallographically independent Sn atom (Wyckoff 16*b* general position), four other unique metal positions (M1 and M2 at Wyckoff 16*b* general position, M3 and M4 at Wyckoff 8*a* position with 2-fold symmetry) randomly occupied by Ga and Ge atoms

in the ratio of Ga:Ge = 2:1, and six unique S atoms (all at Wyckoff 16*b* general position).

Figure 2 illustrates the coordination environments of cations. The Ga and Ge atoms are disordered over four metal sites (M1, M2, M3, and M4) , and they are all tetrahedrally coordinated to four S atoms with Ga/Ge–S distances from 2.214(2) to 2.299(2) Å (Table 2), which are usual compared with those of 2.1801(1) to 2.197(1) Å for Ge–S in $Li_2In_2GeS_6$,[33] 2.180(2) to 2.239(2) Å for Ge–S in $KBiGeS_4$,[34] 2.212(1) to 2.239(1) Å for Ga–S in $BaGa_2SiS_6$,[35] 2.212(1) to 2.239(1) Å for Ga–S in Ba_2NdGaS_5[36] and 2.2427(14) to 2.264(2) Å for Ga/Ge–S in $BaGa_2GeS_6$,[37] and 2.219(3) to 2.258(3) Å for Ga/Ge–S in $Li_2Ga_2GeS_6$.[38] The Sn atom is connected with five S atoms in distorted square pyramid with Sn–S distances from 2.707(2) to 3.227(2) Å (Table 2), which are comparable with those of Sn^{2+} in similar environment (2.665(2) to 3.290(2) Å in Sn_2S_3 [39] and 2.654(19) to 2.992(17) Å in $SnGa_4S_7$).[22] Considering the bonding characteristics in the structure, the oxidation states of 2+, 4+, 3+, and 2− can be attributed to Sn, Ge, Ga and S, respectively and the charge balance can be achieved in this way.

As shown in the Figure 3, the $M1S_4$ tetrahedra and SnS_5 distorted square pyramids connect each other alternately via corner-sharing to form a $^{\infty}_{1}[SnM1S_6]$ chain parallel to the *b* direction (Figure 3A); the $M3S_4$ and $M4S_4$ tetrahedra are joined together via corner-sharing forming one dimensional $^{\infty}_{1}[MS_3]$ (M = M3, M4) chains along *b* direction (Figure 3B). Then two $^{\infty}_{1}[SnM1S_6]$ chains and one $^{\infty}_{1}[MS_3]$ (M = M3, M4) chains further aggregate into a set of complex chains along *b* direction

(Figure 3C). As shown in Figure 4, the complex chains thus formed are connected to each other via the $M2S_4$ tetrahedra, resulting in a three-dimensional framework, within which nearly rectangular-shaped empty channels exist.

Although $SnGa_2GeS_6$ has similar stoichiometry as the previously reported $BaGa_2GeS_6$ compound, the two crystallize in different structure types in different space groups and with strikingly different cell parameters (a = 45.366(9) Å, b = 7.2288(14) Å, c = 11.607(2) Å and Z = 16 in space group *Fdd2* for $SnGa_2GeS_6$ compared with a = 9.5967(11) Å, b = 9.5967(11) Å, c = 8.671(2) Å and Z = 3 in space group *R3* for $BaGa_2GeS_6$.[36]) Such differences may result largely from the different coordination preference between Ba and Sn. For $SnGa_2GeS_6$, Sn is covalently-coordinated to a distorted square-pyramid of five S atoms owing to the stereochemical activity of electron lone pair. The SnS_5 square-pyramids are joined to MS_4 (M = Ga, Ge) alternately forming chains along b direction, which in turn become a part of the three-dimensional framework, leaving empty rectangular-shaped channels in the structure. However, the Ba−S interaction in $BaGa_2GeS_6$ was mostly ionic in character with no orientation preference, leading to a coordination environment of twelve S atoms in a more "spherical" geometry for Ba.[36] Further, the three-dimensional framework in $BaGa_2GeS_6$ is formed by the MS_4 (M = Ga, Ge) tetrahedra only, and the channels within the framework are not empty but occupied by the Ba cations.

SHG Measurement

The SHG signal intensity of $SnGa_2GeS_6$ with the use of the 2090 nm laser as the fundamental wavelength was about one fourth that of $AgGaS_2$ with similar particle size（Figure 5）. Considering the large NLO coefficient of $AgGaS_2$ (d_{36} = 13 pm V^{-1}), the modest NLO coefficient of $SnGa_2GeS_6$ may be estimated to be 3.2 pm/V, which is larger than those of most borates and halides, such as β-BaB_2O_4 (d_{22} (1064 nm) = 2.2 pm V^{-1}),[40] LiB_3O_5 (d_{32} (1064 nm) = 0.85 pm V^{-1}),[41] $CsGeCl_3$ (d_{15} (cal.) = 1.1 pm V^{-1}),[42] $NaSb_3F_{10}$ (d_{33} (cal.) = −0.83 pm V^{-1})[42]

The modest NLO response of $SnGa_2GeS_6$ may be explained based on the macroscopic arrangement of the two kinds of microscopic NLO-active building blocks, i.e. the SnS_5, and MS_4 (M = Ga, Ge) units in the structure. Figure 6 illustrates the overall arrangement of the SnS_5 square pyramids themselves：Although they are almost parallelly aligned in a pseudo chain along the *c* direction, the orientation of adjacent such pseudo chains are tilted to each other at large degree, which is unfavorable for generating large NLO response. As for the MS_4 (M = Ga, Ge) tetrahedra, their packing density in $SnGa_2GeS_6$, as shown by the empty channels in the structure, is obviously smaller than that of the AgS_4 and GaS_4 tetrahedra in $AgGaS_2$. Consequently, the unfavorable macroscopic arrangements of the SnS_5 square pyramids and the MS_4 (M = Ga, Ge) tetrahedra lead to only modest NLO response for $SnGa_2GeS_6$.

Experimental Band Gap

The UV-vis-NIR diffuse reflectance spectrum (Figure 7) shows two optical

transitions, one at about 1.12 (2) eV and the other at about 2.04 (2) eV, which may be explained according to the following electronic structure calculation results. The 1.12 eV transition is due to electron transfer from the valence band to a very narrow band above the Fermi level, while the 2.04 eV transition, which is consistent with the dark red color of crystal, may be explained as electron transfer from the valence band to a much wider conduction band. This band gap is obviously smaller than that of the related $BaGa_2GeS_6$ compound (3.23 eV). The difference may also be explained based on the following electronic structure calculations.

Electronic Structure Calculation

The electronic band structure and DOS/PDOS of the $SnGa_2GeS_6$ crystal are displayed in Figure 8. At about 1.0 eV above the Fermi level, there is a very narrow band mainly composed of Ga 4*s*, Ge 4*s,* and Ge 4*p* orbitals. Then at about 2.0 eV above the the Fermi level, a much wider conduction band is found, which mainly consists of Sn 5*p* , Ga 4*p*, and Ge 4*p* and S 3*p* orbitals. The electron transfers from the valence band to these two bands may account for the two optical transitions observed in the diffuse reflectance spectrum. It should be emphasized that the states on both sides of the band gap are mainly composed of the orbitals from the $[SnS_5]$, $[GeS_4]$ and $[GaS_4]$ groups, which hence mainly determine the optical properties of the $SnGa_2GeS_6$ crystal.[45]

In comparison, for $BaGa_2GeS_6$, The top of the VB and the bottom of CB is mainly occupied by the *p* orbitals of Ge (*4p*), Ga (*4p*) and S (*3p*), with negligible

contribution from Ba atoms. Such different electronic structure characteristics may explain the large difference in the band gaps of these two compounds. It can be seen that Sn-containing compounds distinguish from the related Ba-containing compounds in the crystal structure, physical properties and electronic structure, as a result of the stereochemical activity of the lone pair electrons and the more covalent nature of the Sn–S bonding

Conclusion

In summary, a new Sn-containing chalcogenide, $SnGa_2GeS_6$, has been isolated. It belongs to the orthorhombic space group *Fdd2* and adopts a new structure type with the $Sn^{2+}S_5$ square-pyramids and the MS_4 (M= Ga, Ge) tetrahedra as the basic building units. These SnS_5 square-pyramids and the MS_4 (M= Ga, Ge) tetrahedra are connected to generate a three-dimensional framework with empty rectangular shape channels inside. Although SnS_5 square-pyramids and the MS_4 (M = Ga,Ge) tetrahedra are both microscopic-NLO active units, their macroscopic packing in the structure, including the relative orientation and the packing density, are unfavorable for achieving large NLO response. As a result, the compound exhibits a powder second harmonic generation intensity at 2 μm that is about one-fourth that of the benchmark material $AgGaS_2$. Based on UV-vis-NIR spectroscopy measurement and the electronic structure calculations, $SnGa_2GeS_6$ possesses two optical transitions as a result of the electron transfer from the valence band to a very narrow band and to a much wider conduction band above the Fermi Level, respectively. The synthetic

method, structural characteristics, and the structure-property relationship of $SnGa_2GeS_6$ may provide interesting information for future exploration of IR NLO materials.

Acknowledgments

This research was supported the National Natural Science Foundation of China (No.s 91122034, 51472251, and 21271178).

References

1. D. W. Lee, S. J. Oh, P. S. Halasyamani and K. M. Ok, *Inorg. Chem.*, 2011, **50**, 4473.
2. S. Strobel and T. Schleid, *J. Alloys Compd.*, 2006, **418**, 80.
3. D. L. Gray, L. A. Backus, H. A. Krug von Nidda, S. Skanthakumar, A. Loidl, L. Soderholm and J. A. Ibers, *Inorg. Chem.*, 2007, **46**, 6992.
4. J. H. Yeon, S. H. Kim and P. S. Halasyamani, *J. Chem. Crystallogr.*, 2011, **41**, 328.
5. T. K. Bera, J. I. Jang, J. B. Ketterson and M. G. Kanatzidis, *J. Am. Chem. Soc.*, 2009, **131**, 75.
6. Y. Wu and W. Bensch, *Inorg. Chem.*, 2009, **48**, 2729.
7. W. G. Zhang and P. S. Halasyamani, *Cryst. Growth Des.*, 2012, **12**, 2127.
8. S. P. Guo, G. C. Guo and J. S. Huang, Sci. *China Ser. B-Chem.*, 2009, **52**, 1609.
9. K. Luo, T. T. Tran, P. S. Halasyamani and M. A. Hayward, *Inorg. Chem.*, 2013, **52**, 13762.
10. I. Chung and M. G. Kanatzidis, *Inorg. Chem.*, 2011, **50**, 412.
11. G. B. Jin, E. S. Choi, R. P. Guertin, C. H. Booth and T. E. Albrecht-Schmitt, *Chem. Mater.*, 2011, **23**, 1306.
12. A. Choudhurya, L. A. Polyakova, I. Hartenbach, T. Schleid and P. K. Dorhout, *Z. Anorg. Allg. Chem.*, 2006, **632**, 2395.

13. M. A. Eberle, J. M. Babo and T. Schleid, *Z. Naturforsch. B*, 2014, **69**, 851.

14 A. Choudhury, F. Grandjean, G. J. Long and P. K. Dorhout, *Inorg. Chem.*, 2012, **51**, 11779.

15. J. A. Brant, D. J. Clark, Y. S. Kim, J. I. Jang, J. H. Zhang and J. A, Aitken, *Chem. Mater.,* 2014, **26**, 3045.

16. M. Daszkiewicz, L. D. Gulay and V. Y. Shemet, *Acta Crystallogr. B*, 2008, **64**, 172.

17. J. W. Lekse, M. A. Moreau, K. L. McNerny, J. Yeon, P. S. Halasyamani and J. A. Aitken, *Inorg. Chem.*, 2009, **48**, 7516.

18. J. A. Aitken, J. W. Lekse, J. L. Yao and R. Quinones, *J. Solid State Chem.*, 2009, **182**, 141.

19. Z. Z. Luo, C. S. Lin, W. D. Cheng, H. Zhang, W. L. Zhang and Z. Z. He, *Inorg. Chem.*, 2013, **52**, 273.

20. Z. S. Lin, L. Chen, L. M. Wang, J. T. Zhao and L. M. Wu, *Adv. Mater.*, 2013, **25**, 4800.

21. K. Feng, X. X. Jiang, L. Kang, W. L. Yin, W. Y. Hao, Z. S. Lin, J. Y. Yao, Y. C. Wu and C. T. Chen, *Dalton Trans.*, 2013, **42**, 13635.

22. Z. Z. Luo, C. S. Lin, H. H. Cui, W. L. Zhang, H. Zhang, Z. Z. He and W. D. Cheng, *Chem. Mater.*, 2014, **26**, 2743.

23. CrystalClear. Rigaku Corporation: Tokyo, Japan, 2008.

24. G. M. Sheldrick, *Acta Crystallogr. A*, 2008, **64**, 112.

25. S. K. Kurtz and T. T. Perry, *J. Appl. Phys.*, 1968, **39**, 3798.

26. M. C. Payne, M. P. Teter, D. C. Allan, T. A. Arias and J. D. Joannopoulos, *Rev. Mod. Phys.*, 1992, **64**, 1045.

27. S. J. Clark, M. D. Segall, C. J. Pickard, P. J. Hasnip, M. J. Probert, K. Refson and M. C. Payne, *Z. Krist.*, 2005, **220**, 567.

28. W. Kohn, *Rev. Mod. Phys.*, 1999, **71**, 1253.

29. D. M. Ceperley and B. J. Alder, *Phys. Rev. Lett.*, 1980, **45**, 566.

30. J. S. Lin, A. Qteish, M. C. Payne and V. Heine, *Phys. Rev. B*, 1993, **47**, 4174.

31. H. J. Monkhorst and J. D. Pack, *Phys. Rev. B*, 1976, **13**, 5188.

32. B. G. Pfrommer, M. Cote, S. G. Louie and M. L. Cohen, *J. Comput. Phys.*, 1997, **131**, 233.

33. W. L. Yin, K. Feng, W. Y. Hao, J. Y. Yao and Y. C. Wu, *Inorg. Chem.*, 2012, **51**, 5839.

34. D. J. Mei, Z. S. Lin, L. Bai, J. Y. Yao, P. Z. Fu and Y. C. Wu, *J. Solid State Chem.*, 2010, **183**, 1640.

35. W. L. Yin, K. Feng, R. He, D. J. Mei, Z. S. Lin, J. Y. Yao and Y. C. Wu, *Dalton Trans.*, 2012, **41**, 5653.

36. K. Feng, Y. G. Shi, W. L. Yin, W. D. Wang, J. Y. Yao and Y. C. Wu, *Inorg. Chem.*, 2012, **51**, 11144.

37. X. S. Lin, Y. F. Guo and N. Ye, *J. Solid State Chem.*, 2012, **195**, 172.

38. Y. Kim, I. S. Seo, S. W. Martin, J. Baek, P. S. Halasyamani, N. Arumugam and H. Steinfink, *Chem. Mater.*, 2008, **20**, 6048.

39. M. Cruz, J. Morales, J. P. Espinos, J. Sanzc, *J. Solid State Chem.*, 2003, **175**,

359.

40. I. Shoji, H. Nakamura, K. Ohdaira, T. Kondo, R. Ito, T. Okamoto, K. Tatsuki and S. Kubota, *J. Opt. Soc. Am. B*, 1999, **16**, 620.

41. D. A. Roberts, *IEEE J. Quantum Electron.*, 1992, **28**, 2057.

42. L. Kang, D. M. Ramo, Z. S. Lin, P. D. Bristowe, J. G. Qin and C. T. Chen, *J. Mater. Chem. C*, 2013, **1**, 7363.

43. M. H. Lee, C. H. Yang and J. H. Jan, *Phys. Rev. B*, 2004, **70**, 235110.

Figure captions

Figure 1 Powder x-ray diffraction pattern of $SnGa_2GeS_6$.

Figure 2 Coordination environments of all cations in $SnGa_2GeS_6$.

Figure 3 Chains in $SnGa_2GeS_6$ the structure : (A) $^{\infty}_{1}[SnM1S_6]$ chain; (B) $^{\infty}_{1}[MS_3]$ (M = M3, M4) chain; (C) complex chain formed by $^{\infty}_{1}[SnM1S_6]$ and $^{\infty}_{1}[MS_3]$ (M = M3, M4) chains

Figure 4 Unit cell of the $SnGa_2GeS_6$ structure.

Figure 5 Oscilloscope traces of SHG signals for $SnGa_2GeS_6$ with $AgGaS_2$ as a reference at a particle size of 80−100 μm.

Figure 6 Macroscopic packing of SnS_5 polyhedra in the structure.

Figure 7 Diffuse reflectance spectrum of $SnGa_2GeS_6$.

Figure 8 The band structure (a) and DOS/PDOS (b) of the $SnGa_2GeS_6$ crystal.

Table 1 Crystal data and structure refinements for $SnGa_2GeS_6$

	$SnGa_2GeS_6$
fw	523.08
T(K)	298
a (Å)	45.366(9)
b (Å)	7.2288(14)
c (Å)	11.607(2)
Space group	*Fdd2*
V(Å^3)	3806.4(13)
Z	16
ρ_c (g/cm^3)	3.651
μ(cm^{-1})	12.561
$R(F)$ [a]	0.0416
$R_W(F_o^2)$ [b]	0.1044

[a] $R(F) = \sum \| \|F_o\| - \|F_c\| \| / \sum |F_o|$ for $F_o^2 > 2\sigma(F_o^2)$. [b] $R_w(F_o^2) = \{\sum [w(F_o^2 - F_c^2)^2] / \sum wF_o^4\}^{1/2}$ for all data. $w^{-1} = \sigma^2(F_o^2) + (zP)^2$, where $P = (\mathrm{Max}(F_o^2, 0) + 2F_c^2)/3$.

Table 2 Selected interatomic distances (Å) for $SnGa_2Ges_6$

	$SnGa_2GeS_6$
Sn—S1	2.707(2)
Sn—S6	2.782(2)
Sn—S4	2.809(2)
Sn—S5	2.3174(23)
Sn—S3	3.2274(23)
Ga1—S2	2.241(2)
Ga1—S5	2.252(2)
Ga1—S6	2.2525(19)
Ga1—S1	2.273(2)
Ga2—S2	2.214(2)
Ga2—S5	2.227(2)
Ga2—S3	2.235(2)
Ga2—S3	2.250(2)
Ge1—S6×2	2.285(2)
Ge1—S4×2	2.287(2)
Ge2—S4×2	2.296(2)
Ge2—S1×2	2.299(2)

Figure 1 Powder x-ray diffraction pattern of $SnGa_2GeS_6$.

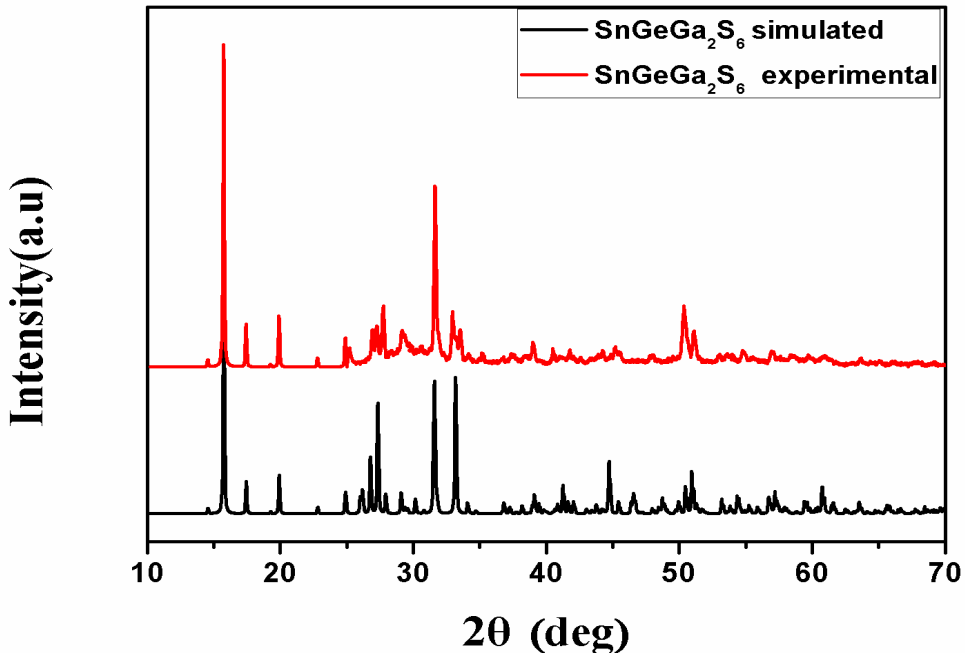

Figure 2 Coordination environments of all cations in $SnGa_2GeS_6$.

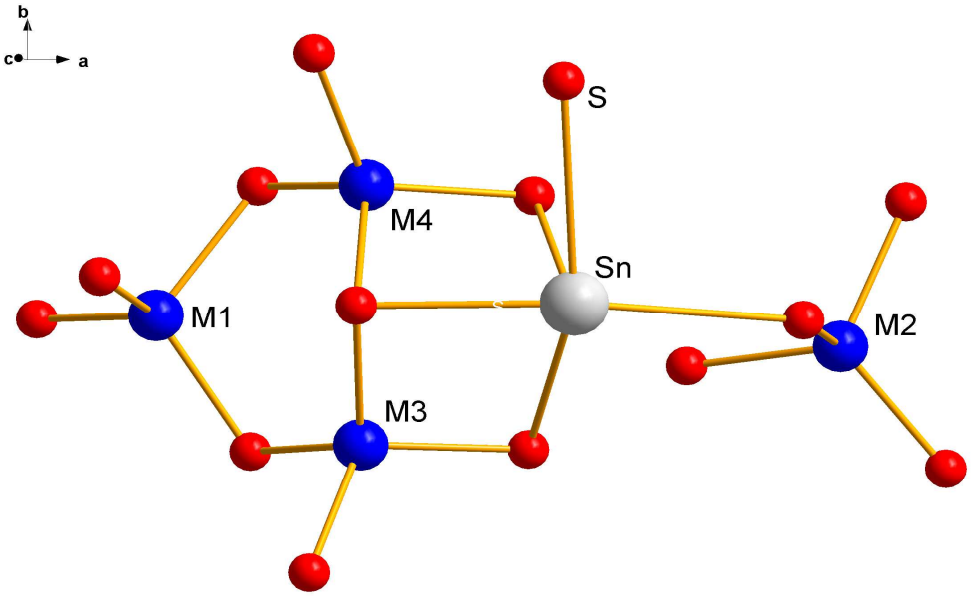

Figure 3 Chains in $SnGa_2GeS_6$ the structure : (A) $^{\infty}_{1}[SnM1S_6]$ chain; (B) $^{\infty}_{1}[MS_3]$ (M = M3, M4) chain; (C) complex chain formed by $^{\infty}_{1}[SnM1S_6]$ and $^{\infty}_{1}[MS_3]$ (M = M3, M4) chains

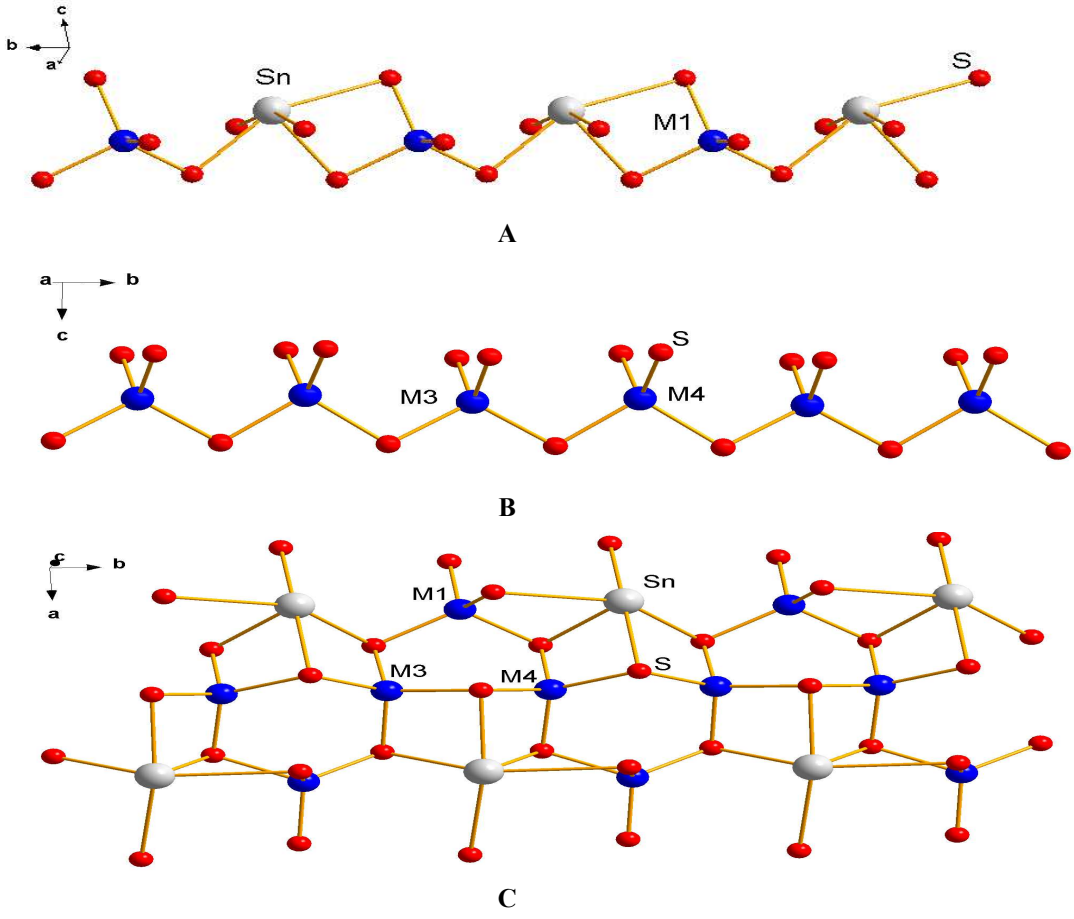

Figure 4 Unit cell of the $SnGa_2GeS_6$ structure.

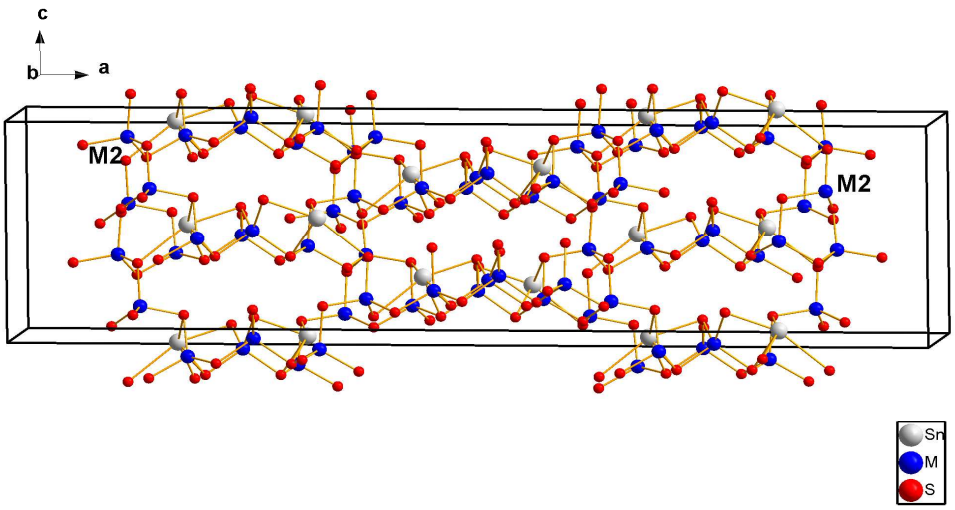

Figure 5 Oscilloscope traces of SHG signals for $SnGa_2GeS_6$ with $AgGaS_2$ as a reference at a particle size of 80−100 μm.

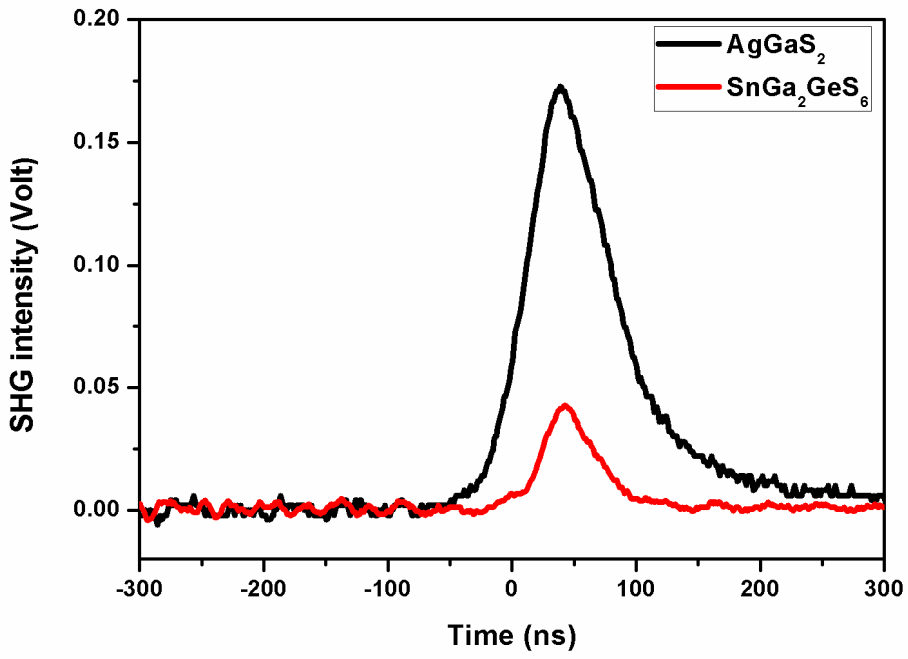

Figure 6 Macroscopic packing of SnS_5 polyhedra in the structure.

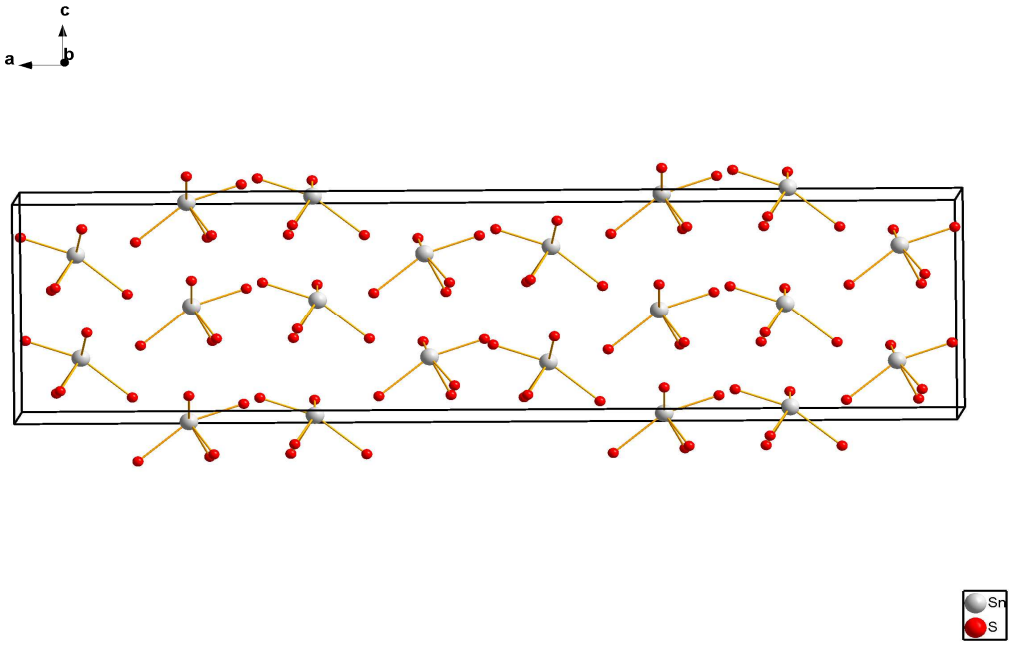

Figure 7 Diffuse reflectance spectrum of $SnGa_2GeS_6$.

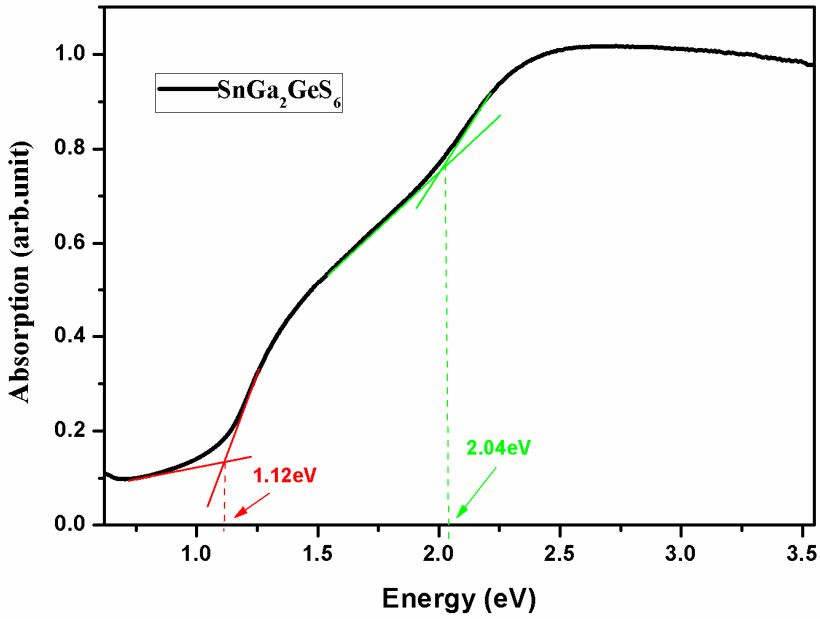

Figure 8 The band structure (a) and DOS/PDOS (b) of the $SnGa_2GeS_6$ crystal.

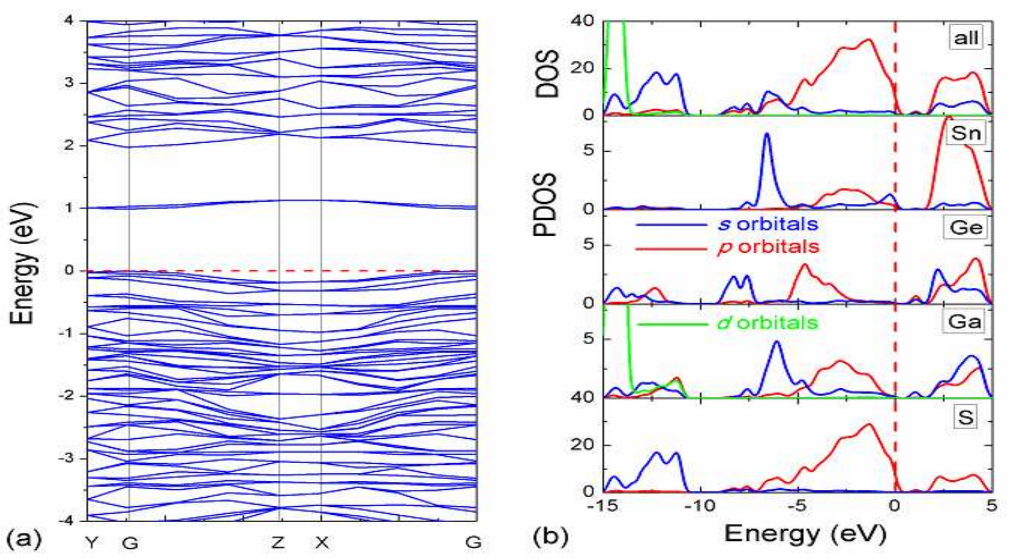

Table of Contents Entry

$SnGa_2GeS_6$ possesses a powder second harmonic generation response and a band gap of 2.04 eV.